LETTER

Signatures of two-dimensional transport in superconducting nanocrystalline boron-doped diamond films

To cite this article: Christopher Coleman and Somnath Bhattacharyya 2018 *EPL* **122** 57004

A Letters Journal Exploring the Frontiers of Physics

June 2018

EPL, **122** (2018) 57004 www.epljournal.org
doi: 10.1209/0295-5075/122/57004

Signatures of two-dimensional transport in superconducting nanocrystalline boron-doped diamond films

Christopher Coleman and Somnath Bhattacharyya[(a)]

Nano-scale Transport Physics Laboratory and DST/NRF Centre of Excellence in Strong Materials, University of the Witwatersrand - Private Bag 3, WITS 2050, Johannesburg, South Africa

received 5 March 2018; accepted in final form 22 June 2018
published online 16 July 2018

PACS 74.20.Mn – Nonconventional mechanisms
PACS 74.25.-q – Properties of superconductors
PACS 74.40.-n – Fluctuation phenomena

Abstract – The possibility of a two-dimensional (2D) phase is investigated in superconducting boron-doped nanocrystalline diamond films. The fluctuation spectroscopy schemes such as the Azlamazov-Larkin (AL) and Lerner-Varlamov-Vinokur (LVV) ones are used to determine the dimensionality crossovers occurring near the superconducting phase transition. It is found that a distinct 2D phase in the fluctuation regime occurs. One of the consequences of the 2D transport is the manifestation of the Berezinskii-Kosterlitz-Thouless (BKT) transition which is verified through both current voltage power law scaling as well as the Halperin-Nelson fitting to the temperature-dependent resistance. The suppression of the BKT transition with applied field is found to be correlated with the decrease of Josephson coupling between grains. The identification of a 2D phase accompanied by the BKT transition highlights the subtle effects of dimensionality in this unique system.

Introduction. – Superconductivity in reduced dimensions are well known to exhibit interesting physics [1], in particular superconductivity in 2D has been investigated with regard to non-trivial topological ordering due to spontaneous time-reversal symmetry breaking [2]. Such non-trivial topological superconductors are generally described in terms of odd-parity and spinless wave function [3] and have been observed experimentally only in a handful of materials [4]. Since topologically protected states are expected to be useful for decoherence robust qubits [5], much research is directed at identifying potential materials offering such exotic low-dimensional phases.

The theoretical models developed for identifying the dimensionality of superconductors have been extensively used in both single-crystal and polycrystalline materials, proving to be invaluable in helping to classify materials so that this area of analysis is sometimes referred to as "fluctuoscopy" [6]. The main theoretical model was developed by AL [7] to explain how the formation of finite lifetime Cooper pair excitations above, but near to, the mean-field critical point contribute to the excess conductivity. The model allowed for the determination of the dimensionality of the transport channels in a range of superconducting materials [8–10].

More recently the effects of granularity on the dimensionality of the transport channels have been suggested [11]. The granularity allows for charging and additional scattering effects and offers a suitable system for studies of the interplay of electron correlations and mesoscopic disorder. LVV suggested a characteristic scaling scheme for granular superconductors which is based on the evolution of the temperature-dependent Ginzburg-Landau coherence length driven by inter- and intra-grain coupling [11].

This generalized model predicted that granular superconducting media would follow a series of dimensionality crossovers starting from a 3D regime within the grain, a quasi-0D (q-0D) regime where the coherence length is comparable to the grain size and finally a 3D regime as the coherence length increases beyond the grain size and Josephson coupling between grains occurs. This model has recently been applied to superconducting boron-doped diamond [12]. Although the predicted result of an upturn in resistance due competition between the suppression of single-electron tunnelling and coherent charge transfer of Cooper pairs was not reported, the dimensionally

[(a)]E-mail: Somnath.Bhattacharyya@wits.ac.za

crossover predicted by the model has indeed been observed [12]. In this work we investigate more deeply the excess conductivity region between the q-0D and 3D transition and show that the smoothness of the transition is due to a conductivity region that follows the scaling predicted for 2D transport. This indicates the presence of a 2D phase that occurs just before the Josephson coupling becomes significant and intergrain transport occurs. This observation is explained in the light of the complex microsctructure of this system. As superconducting diamond has been classified as a type-two superconductor it bears many similarities with the layered cuprates. The intergranular subsystem is believed to lead to a superconductor-insulator-superconductor junction superlattice where the interfacial boundary region and weak coupling between grains are likely responsible for the two-dimensionality.

We present an interesting manifestation of this 2D coupled system, the BKT transition in a nanodiamond system. The BKT transition is classified as a topological phase transition as the long-range behaviour of the system is determined by its topology [13] instead of spontaneous breaking of underlying symmetries that describe the system. During the transition thermal excitations of topological defects in 2D (vortex and antivortex pairs) bind together allowing for the long-range order. The experimental characteristics of the BKT transition are well documented and generally easily identified through analysis of temperature-dependent transport properties [13–16]. In this study we present the temperature dependence of both resistance and voltage-current (V-I) characteristics to verify the occurrence of the BKT transition which we relate to the anomalous bosonic insulation (BI) phase reported for this material [17–19].

Methods. – The diamond samples used in this study were synthesized using a microwave plasma enhanced chemical vapour deposition technique on quartz substrates. The grain size (30 nm to 70 nm) can be controlled by varying the methane-to-hydrogen ratio from 2.5% to 5% CH_4 in H_2 with trimethylborane (TMB) as a dopant precursor (∼4000 ppm in the films). Samples have been named according to the CH_4/H_2 ratio used during the synthesis of respective samples, *i.e.*, B2.5, B4 and B5. The data presented in this article are from the same sample (B5) and data from the other samples (B2.5 and B4) are presented in the supplementary material `Supplementarymaterial.pdf` (SM). Although the boron precursor gas was kept constant during the synthesis of the films, it has been shown that the boron concentration increases with decreasing grain size16. Scanning electron microscopy was used to determine the average grain size of the films. The films are typically 300 nm thick. The existence of superconductivity is confirmed by measuring the resistance as a function of temperature as well as at various magnetic fields and fixed bias currents. Transport measurements were performed in the van der Pauw

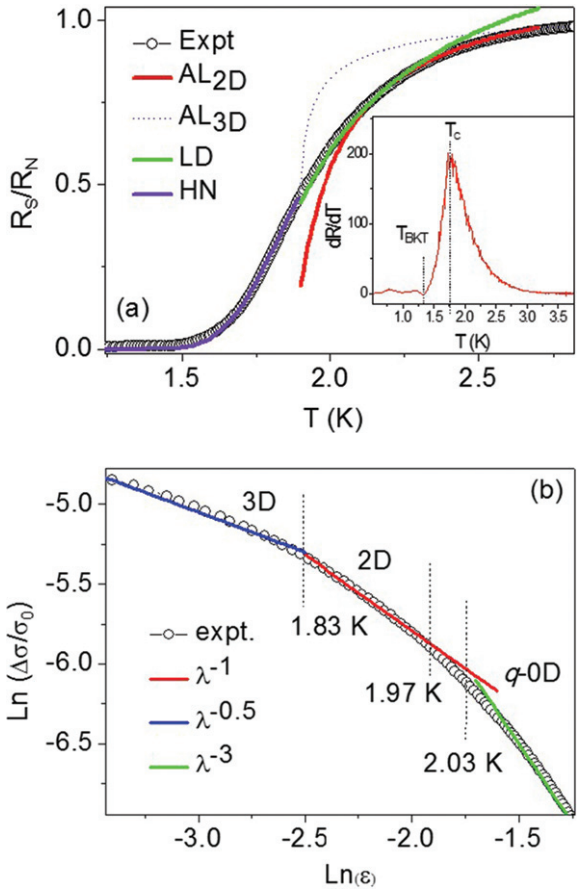

Fig. 1: (Colour online) (a) The temperature dependence of the sheet resistance normalized to the resistance in the normal state. The curvature of the transition can be best fit to fluctuation models taking into account 2D to 3D crossover. The mean-field critical point used in the fitting is derived from the peak position in the derivative of the temperature-dependent resistance (dR/dT) as shown in the inset. The transition region was also fitted to the Lawerence-Doniach (LD) and Halperin Nelson (HN) theory. (b) The crossover from the quasi-0D to 2D to 3D excess conductivity regimes is clearly indicated as a function of the reduced temperature scale. Although the intermediate regime is small, this region of excess conductivity between the q-0D and 3D follows the expected critical exponent for an intermediate state. The relevant temperatures for the crossover in dimensionality have been included.

configuration using a closed-cycle cryo-free system with lock-in amplifier and nanovoltmeter. Magnetic fields were applied perpendicular to the film surface. The temperature stability was better than 10% at 300 mK. All samples undergo a metal-superconductor transition with critical temperatures in the range 1.2 K–3.6 K.

Results. – As shown in fig. 1, the superconducting transition of the diamond films shows a broad smooth transition instead of a sharp downturn to the superconducting state. This is typical in superconducting materials that show dimensional transport channel crossover. In order to investigate such an occurrence, the AL equations

have been used in a range of materials including both thin films and bulk crystals. In this scheme [6,7] the fluctuation-induced conductivity can be represented in 2D as well as 3D according to

$$\Delta\sigma_{2D} = \frac{e^2}{16\hbar d}\frac{T}{T-T_C}, \tag{1}$$

$$\Delta\sigma_{3D} = \frac{e^2}{32\hbar\xi(0)}\left(\frac{T}{T-T_C}\right)^{1/2}. \tag{2}$$

Or in a more compact and generalized form as

$$\Delta\sigma = A\varepsilon^{-\lambda}, \tag{3}$$

where A is a coefficient taking on the respective values for 2D or 3D depending on the coherence length $\xi(0)$ as well as intergrain separation or interlayer spacing (d) as given in eqs. (1) and (2). The reduced temperature is described as $\varepsilon = (T - T_C)/T$. The exponent λ is dependent on the dimensionality of the transport and takes on values of -1.0 and -0.5 for 2D and 3D, respectively. Shown in fig. 1(a) is the application of the AL equations, where the red line is a fit to the 2D AL equation and the dotted line a fit to the 3D equation. As can be seen, the 3D equation does not fit the data set particularly well, and the 2D fit can be applied to some extent but breaks down upon approaching the mean-field critical point, here defined as the peak in the temperature-dependent derivative of the resistance (fig. 1(a), inset). This clearly demonstrates a crossover in the dimensionality and, thus, an additional fitting with the Lawrence-Doniach (LD) model [20] that takes account of the Josephson coupling between 2D planes was used and it is given by

$$\Delta\sigma = \frac{e^2}{16\hbar d}\varepsilon^{-1}\left[1+\left(\frac{2\xi(0)}{d}\right)^2\right]^{-1/2}. \tag{4}$$

The LD fitting is indicated by the green line in fig. 1(a) and shows a good correlation to the data particularly near T_C. To better understand the various transport dimensionalities within the fluctuation-induced regimes the excess conductivity is plotted as a function of the reduced temperature, as shown in fig. 1(b). The crossover from the quasi-0D to the 3D regime previously described [13] is clearly interrupted by a region following the 2D critical exponent of $\lambda = 1$. This 2D region is furthermore believed to be significant as the 2D scaling occurs across most of this intermediate temperature regime and was consistently observed between samples. As this system is composed of a complex microstructure where superconducting diamond grains are separated from each other by the intergranular sublattice system, it is believed that the weak Josephson coupling ensures that the Cooper pairs are confined even as the pair size (coherence length) increases beyond the diameter of the grain, in order to accommodate the growing Cooper pair size the wave function exploits on the surface of the diamond crystallites leading to a skin-effect before intergranular coupling occurs.

One of the most striking features of the 2D phase is the manifestation of an apparent BKT transition [21,22]. The hallmark feature of the BKT transition is the power law behaviour of V-I characteristics, which is related to the universal jump in the superfluid density due to vortex-antivortex binding upon reaching the BKT transition temperature (TBKT). This jump in superfluid density is determined through analysis of the power law exponent describing the V-I characteristics. The BKT transition is expected when the slope of the V-I curve is steep enough to yield an exponent with value of $\alpha = 3$, *i.e.*, $V \sim I^3$.

This has indeed been observed in a range of samples (see SM), and occurs at approximately 1.3 K for the particular film represented in fig. 2(a) as indicated by the dashed line. The occurrence of the BKT transition was also determined to be extremely sensitive to the applied field, when evaluating that the power law behaviour of the V-I characteristics the BKT transition was completely suppressed at fields as low as 0.2 T. Figure 2(b) shows the V-I curves for the same sample as that represented in fig. 2(a), this time, however, at an applied field of 1 T.

There is a substantial change in the curvature and the power exponent is not observed to reach a value of 3 in the experimentally accessible temperature range. Figure 2(c) shows the temperature dependence of the exponent, where a stark difference between zero and small applied fields can be seen. As mentioned above, only when no field is applied can the BKT transition be observed. The BKT transition can also be identified in the temperature-dependent resistance, this is achieved firstly through fitting the normalized resistance to the Halperin-Nelson (HN) formula [14] valid between T_{BKT} and T_C.

$$\frac{R_N}{R} = 1 + \left(\frac{2}{A}\sinh\frac{b}{\sqrt{t}}\right)^2, \tag{5}$$

where A is a coefficient of order 1 and b is related to the temperature difference between T_C and T_{BKT}. This fitting is indicated by the blue solid line in fig. 1(a). The BKT temperature obtained from the HN fitting is the same as that obtained from the V-I analysis (*i.e.*, 1.3 K for the sample presented here). This occurrence of a transition is also demonstrated when plotting the temperature-dependent resistance on a log scale. As shown in fig. 3(a), the resistance then clearly shows a resistive peak feature at the BKT temperature. As before, when the magnetic field is applied, the BKT transition is not observed, as indicated by the absence of the resistive upturn.

Further verification of the BKT transition can be made by comparing the resistance data to predictions of the BKT theory [13,14], *i.e.*, showing that the resistance tail below T_C depends exponentially on the inverse square root of the reduced temperature:

$$ln\left[\frac{R_s(T)}{R_n}\right] = a - bt^{-1/2}, \tag{6}$$

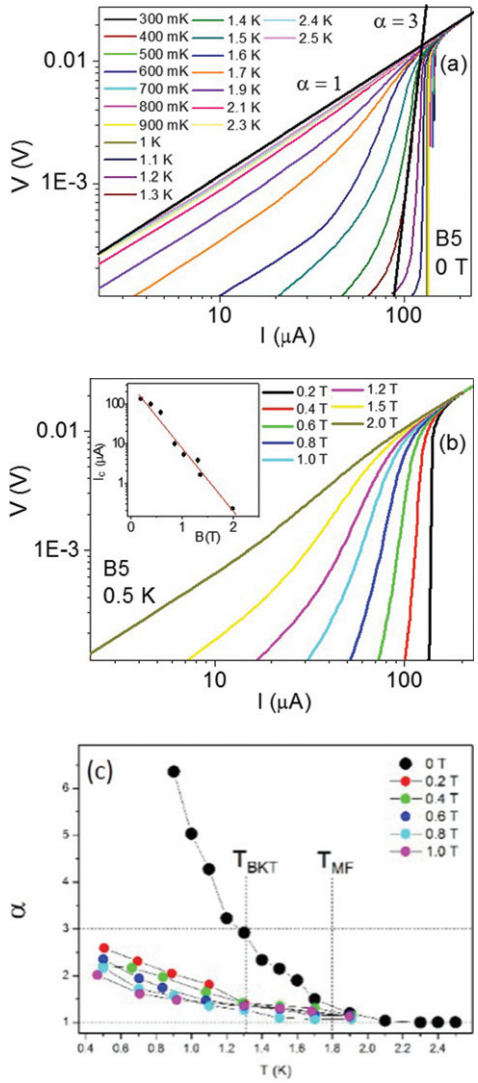

Fig. 2: (Colour online) (a) The power law scaling of the I-V characteristics as a function of temperature at 0 T. The universal jump in superfluid density is indicated by the dashed line. (b) The effect of applying magnetic fields at low temperature, the expected scaling for the BKT transition is not observed at any field above 0.2 T; also indicated in the inset is the power law scaling of the critical current as a function of the applied field. As can be seen, the scaling does not increase to above 3 for the accessible temperature range. (c) The critical exponent defining the power law scaling of I-V as a function of temperature at different applied magnetic fields. The BKT transition is completely suppressed in the accessible temperature range for fields as small as 0.2 T.

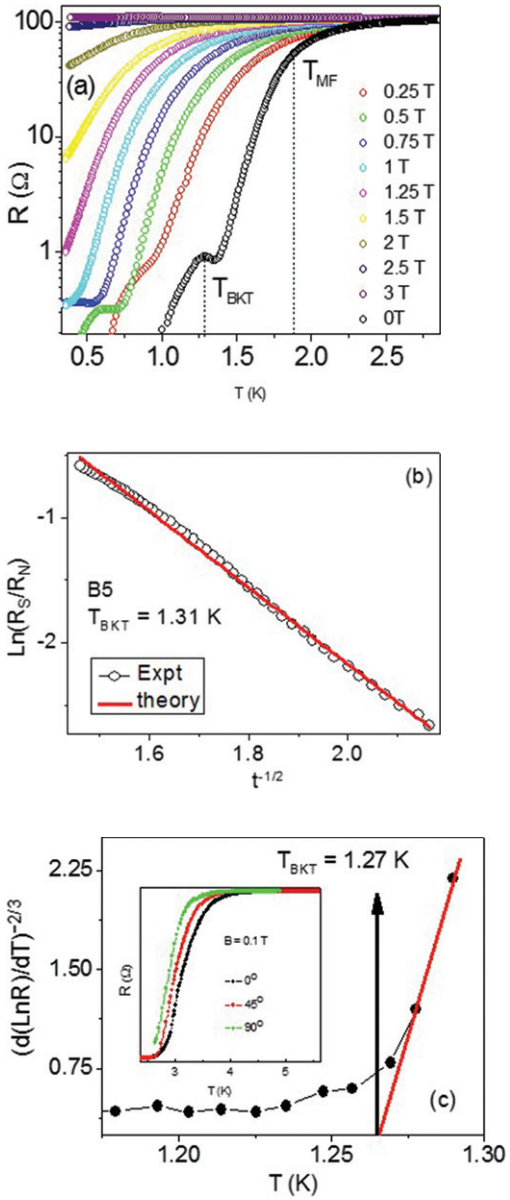

Fig. 3: (Colour online) (a) The evolution of the temperature-dependent resistance as the applied field is increased plotted in log scale. With zero applied field an upward turn and peak in the resistance are clearly seen. The upward turn is not seen in any instance the field is applied. Different scaling relations based on the Halperin-Nelson interpolation formula are presented in (b) yielding a BKT temperature of 1.21 K (b) and 1.27 K (c), indicating consistency within 40 mK. (c) The inset shows temperature-dependent resistance at different orientations of the applied field, a clear change in the transition temperature is observed indicating anisotropic transport.

where a and b are non-universal dimensionless constants. The BKT temperature can also be extracted through analysing the temperature dependence of $\mathrm{d}(\ln R/\mathrm{d}T)^{-2/3}$.

As shown in fig. 3(c), (b) both representations yield a BKT temperature between 1.27 K and 1.31 K, *i.e.*, a deviation of only 40 mK, indicating good consistency between the respective models. Pronounced resistive upturns in this material have been observed before and attributed to the formation of a bosonic insulating phase consisting of localized Cooper pairs due to confinement effects [19], such bosonic insulating phases are well known to lead to a dual charge-BKT transition in low-dimensional systems [23] and Josephson-Junction arrays tuned to the low-coupling regime [24]. The observation of the BKT-transition at the insulating phase thus unifies the bosonic

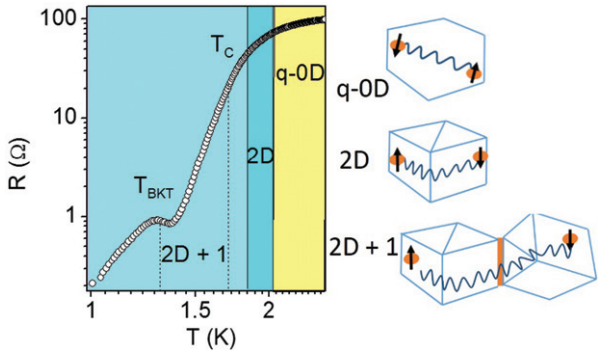

Fig. 4: (Colour online) The temperature-dependent resistance in double log scale, the various temperature regions where dimensionality crossover occurs as determined from the AL and LVV fittings have been indicated. The accompanying images on the right show that the difference between the dimensionality regimes with the q-0D phase has a Cooper pair size comparable to the grain diameter, the intermediate 2D state represented as a surface state around the circumference of the diamond grain and lastly the 2D + 1 phase where grain coupling sets in and Cooper pairs can travel between grains.

insulating phase discovered by Zhang *et al.* [17–19] with other systems exhibiting the bosonic insulating phases.

In order to explain the physical observations presented above we rely on the fluctuation spectroscopy already conducted on boron-doped superconducting diamond [12]. There it was suggested that upon cooling to the superconducting state the system exhibits a 3D to quasi-0D to 3D transition. This crossover was explained in terms of the scaling of the temperature dependence of the Ginzburg-Landau coherence length of the Cooper pairs. As shown in the inset of fig. 3(c) temperature-dependent resistance obtained in applied fields of different orientation has shown shifting of the critical temperature, this is a strong indication of anisotropy related to the dimensionality crossover. At temperatures slightly higher than the T_C the conductivity is dominated by fluctuations due to Cooper pair formation, in this temperature regime the scaling is 3D as the coherence length is less than the grain size and can increase in three spatial dimensions. As the systems is cooled, the coherence length increases until reaching the grain size. This temperature range is called the quasi-0D regime and is characteristic of Cooper pairs localized within the individual grains.

According to the LVV model for granular superconductors [12] the system is then expected to enter the 3D regime (or 2D + 1) as the coherence length increases tunnelling of the Cooper pairs between grains resulting in the 3D behaviour. In this work it is demonstrated that there is evidence suggesting that (at least 300 mK) before this final coupling between grains is reached the system enters into a 2D phase that follows the AL 2D theory.

At temperatures below the mean-field critical point, the observation of the BKT transition, which is the vortex-antivortex binding point, is most likely a result of the Josephson coupling between adjacent grains, similar to the coupling between 2D layers in the high T_C cuprates [25,26]. This crossover in the dimensionality is demonstrated schematically in fig. 4. The suppression of this BKT transition with applied field can be explained as a result of the magnetic-flux lines which propagate along the grain boundaries decreasing the coupling strength between the grains.

Having presented evidence for both the 2D nature and the topological excitations causing the BKT transition, it is quite plausible to expect a topological phase. The occurrence of topologically protected phases has been theoretically predicted and experimentally observed in a wide range of low-dimensional carbon and boron materials [27–30]. In fact, very recently Fermi arcs were observed in the Fermi surface of a low-dimensional boron called borophene [31]. Recent XRD and Raman spectroscopy studies based on polycrystalline boron-doped diamond also suggested the existence of structurally arranged bilayer boron sheets [32] and since weak surface superconductivity in single-crystal bulk boron-doped diamond [33] has already been observed, it is not difficult to imagine the existence of a topological 2D phase in nanocrystalline films presented here, especially considering the enhanced confinement effects already reported for this system.

Conclusion. – We have shown through the AL and LVV scaling analysis that a distinct 2D phase is observable in the temperature-dependent resistance. Although the LVV scaling has been investigated before in superconducting boron-doped diamond, this is the first investigation of the 2D phase which was determined to set in before intergranular coupling occur. The 2D phase is expected to have implications on the transport of the system. We have verified this by identifying the occurrence of the BKT transition at temperatures below the mean-field critical point just before global coherence and the zero resistance occur. This has been achieved through both current-voltage power law scaling analysis as well as analysis of the temperature-dependent resistance using the Halperin-Nelson equation. It was also observed that the BKT transition was suppressed drastically with the application of magnetic field. As the BKT transition is due to topological excitations (vortex-antivortex pairs) this phenomenon is a strong indication that topological distinct phases occur in this system. Although more research is required to determine whether the phase is trivial or not. This study highlights the similarity between the boron-doped diamond and layered high-T_C materials and shows how the combination of both granularity and the intergranular subsystem can lead to low-dimensional confinement effects.

* * *

SB is very thankful to M. Nesládek (Hasselt University) for providing the samples and conducting stimulating discussions. NRF (SA) and CSIR-NLC are acknowledged

for the financial support. This work is conducted under the BRICS multilateral project.

REFERENCES

[1] Brun C., Chren T. and Roditchev D. E., *Supercond. Sci. Technol.*, **30** (2017) 013003G.

[2] Volovik G. E., *JETP Lett.*, **66** (1997) 522Y; Fu L. and Berg E., *Phys. Rev. Lett.*, **105** (2010) 097001.

[3] Qi X.-L. and Zhang S.-C., *Rev. Mod. Phys.*, **83** (2011) 1057.

[4] Sato M. and Ando Y., *Rep. Prog. Phys.*, **80** (2017) 076501.

[5] Hassler F., Akhmerov A. R. and Beenakker C. W. J., *New J. Phys.*, **13** (2011) 095004.

[6] Varlamov A. A., *"Fluctuoscopy" of Superconductors*, in *Fundamentals of Superconducting Nanoelectronics. NanoScience and Technology*, edited by Sidorenko A. (Springer, Berlin, Heidelberg) 2011.

[7] Aslamasov L. G. and Larkin A. I., *Phys. Lett. A*, **26** (1968) 238.

[8] Deutscher G., Goldman A. M. and Micklitz H., *Phys. Rev. B*, **31** (1986) 1679.

[9] Shi J. H., Wang H. S., Wang Y. G., Zhao B. R., Zhoa Y. Y. and Li L., *Solid State Commun.*, **63** (1987) 641.

[10] Lepage Y., McKinnon W. R., Tarascon J. M., Greene L. H., Hull G. W. and Hwang D. M., *Phys. Rev. B*, **35** (1987) 7245.

[11] Lerner I. V., Varlamov A. A. and Vinokur V. M., *Phys. Rev. Lett.*, **100** (2008) 117003.

[12] Klemencic G. M., Fellows J. M., Werrell J. M., Mandal S., Giblin S. R., Smith R. A. and Williams O. A., *Phys. Rev. Mater.*, **1** (2017) 044801.

[13] Kosterlitz J. M. and Thouless J. D., *J. Phys. C: Solid State Phys.*, **6** (1973) 1181.

[14] Halperin B. I. and Nelson D. R., *J. Low Temp. Phys.*, **36** (1979) 599.

[15] Minnhagen P., *Rev. Mod. Phys.*, **59** (1987) 1001.

[16] Ioffe L. B., Feigel'man M. V., Ioselevich A., Ivanov D., Troyer M. and Blatter G., *Nature*, **415** (2002) 503.

[17] Zhang G., Samuely T., Kačmarčík J., Ekimov E. A., Li J., Vanacken J., Szabó P., Huang J., Pereira P. J., Cerbu D. and Moshchalkov V. V., *Phys. Rev. A*, **6** (2016) 064011.

[18] Zhang G., Zeleznik M., Vanacken J., May P. W. and Moshchalkov V. V., *Phys. Rev. Lett.*, **110** (2013) 077001.

[19] Zhang G., Samuely T., Du H., Xu Z., Liu L. *et al.*, *ACS Nano*, **11** (2017) 11746.

[20] Lawrence W. E. and Doniach S., in *Proceedings of the Twelfth International Conference on Low Temperature Physics*, edited by Kanda E. (Keigaku, Tokyo) 1971, p. 361.

[21] Coleman C. and Bhattacharyya S., *AIP Adv.*, **7** (2017) 115119.

[22] Mtsuko D., Coleman C. and Bhattacharyya S., arXiv:1606.06672.

[23] Fisher M. P. A., *Phys. Rev. Lett.*, **65** (1990) 923.

[24] Mooij J. E., van Wees B. J., Geerligs L. J., Peters M., Fazio R. and Schön G., *Phys. Rev. Lett.*, **65** (1990) 645.

[25] Blatter G., Feigel'man M. V., Geshkenbein V. B., Larkin A. I. and Vinokur V. M, *Rev. Mod. Phys.*, **66** (1994) 1125.

[26] Dodgson M. J. W., Geshkenbein V. B. and Blatter G., *Phys. Rev. Lett.*, **83** (1999) 5358.

[27] Gomes K. K., Mar W., Ko W., Guinea F. and Manoharan H. C., *Nature*, **483** (2012) 306.

[28] Weng H., Liang Y., Xu Q., Yu R., Fang Z., Dai X. and Kawazoe Y., *Phys. Rev. B*, **92** (2015) 045108.

[29] Zhai X. and Jin G., *Appl. Phys. Lett.*, **102** (2013) 023104.

[30] Tang P., Zou Z., Wang S., Wu J., Liu H. and Duan W., *RSC Adv.*, **2** (2012) 6192.

[31] Feng B. *et al.*, *Phys. Rev. Lett.*, **118** (2017) 096401.

[32] Polyakov S. N., Denisov V. N., Mavrin B. N., Kirichenko A. N., Kuznetsov M. S., Yu Martyushov S., Terentiev S. A. and Blank V. D., *Nanoscale Res. Lett.*, **11** (2016) 11.

[33] Blank V., Buga S., Bormashov V., Denisov V., Kirichenko A., Kulbachinskii V., Kuznetsov M., Kytin V., Kytin G., Tarelkin S. and Terentiev S., *EPL*, **108** (2014) 67014.